The Flame Structure and Vorticity Generated by a Chemically Reacting Transverse Jet

A. R. Karagozian*
University of California, Los Angeles, California

An analytical model describing the behavior of a turbulent fuel jet injected normally into a cross flow is developed. The model places particular emphasis on the contra-rotating vortex pair associated with the jet and predicts the flame length and shape based on entrainment of the oxidizer by the fuel jet. Effects of buoyancy and density variations in the flame are neglected at present in order to isolate the effects of large-scale mixing. The results are compared with a simulation of the transverse reacting jet in a liquid (acid-base) system. For a wide range of ratios of the cross flow to jet velocity, the model predicts flame length quite well. In particular, the observed transitional behavior in the flame length between $0.0 < U_\infty / U_j < 0.1$, yielding an approximate minimum at the ratio 0.05, is reproduced very clearly by the present model. The transformation in flow structure that accounts for this minimum arises from the differing components of vorticity dominant in the near- and far-field regions of the jet.

Nomenclature

a = radius of vortex core
d = jet orifice diameter
E = entrainment coefficient
h = vortex pair half-spacing
L = characteristic length
R = jet-to-cross-flow velocity ratio
R_L = maximum value of R for which model applies
Re = jet Reynolds number
s_f = flame arc length
t = flow time
t_0 = flow time corresponding to initial conditions at jet orifice
t_* = flow time at which flame ends
U = cross-flow velocity relative to vortex pair
U_∞ = cross-flow velocity
U_j = jet velocity of orifice
u_v = mass-averaged jet velocity
X, Z = flowfield coordinates of vortex pair
X_f, Z_f = flowfield coordinates of flame end
α = stoichiometric mixture ratio (oxidizer/fuel)
Γ_0 = total circulation of each vortex
ν = kinematic viscosity
ν_t = average eddy viscosity
ϕ_v = local angle of orientation of vortex pair

Introduction

THE entrainment and mixing that occurs when a single jet is directed normally into a cross flow has been studied rather extensively over the past few decades, primarily through experiments[1,2] and empirical or semiempirical models.[3,4] If the jet contains a substance that reacts rapidly with the cross stream to form a product, the situation can represent a circular fuel jet burning in a crosswise airstream. This occurs, for example, in industrial gas burners where turbulent diffusion flames are deflected by a cross stream of air. While the local flowfield will be similar to that for the nonreacting fuel jet, a finite flame length will be apparent when sufficient mixing and reactant consumption has taken place.

Broadwell and Breidenthal[5] have investigated this flowfield experimentally using a liquid system in which a circular jet containing a base solution is injected into a water tunnel containing a cross stream of dilute acid. Visualization of the jet takes place by means of a pH indicator, similar to the method used by Weddell to visualize free turbulent fuel jets (recorded in a survey by Hottel and Luce[6]). In both sets of experiments, the reaction's equivalence ratio α (defined as the ratio of the volume of ambient fluid to injected fluid required for products to form) is varied by changing the concentrations of the reactants, so that visible "flame" lengths will depend on α. Broadwell and Breidenthal also describe, by means of scaling laws, a model for the far-field behavior of the flame. Semiempirical modeling of the gaseous turbulent diffusion flame in a cross flow has been performed by Brzustowski[7] based on earlier experimental work on hydrocarbon jets.[8-10] While the model's results are significant in terms of discerning the physical phenomena relevant to the transverse fuel jet, prediction of the flame length at high ratios of the jet to cross-flow velocity is as yet incomplete.

The present study seeks to model analytically the single isothermal transverse fuel jet by identifying some of the characteristics common to reacting and nonreacting transverse jets. In particular, emphasis will be placed on the vortex pair structure that has been observed to dominate both reacting and nonreacting cross sections in the far field. A previously developed[11] vortex model for the single, transverse jet will thus be incorporated, including the reacting chemical species. In addition, the influence of the entrainment of oxidizer and large-scale mixing on the behavior of the fuel jet will be examined so that flame length may be predicted for a wide spectrum of cross-flow-to-jet velocity ratios.

Vortex Model for the Single Transverse Jet

While a detailed description of the vortex model for a single incompressible transverse jet has been described previously,[11] only its pertinent features will be outlined here. The actual jet cross section can be approximated by the recirculation cell of the vortex pair and, considering the vortices to be locally two-dimensional, the jet path is traced by evaluating the motion of the vortex pair. The geometry of the situation is described in Fig. 1, with flow time t parametrizing the vortex curve.

Received Aug. 2, 1985; revision received Dec. 9, 1985.

*Assistant Professor, Department of Mechanical, Aerospace, and Nuclear Engineering.

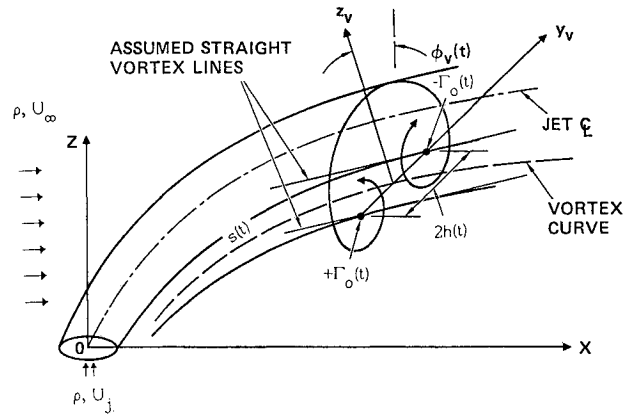

Fig. 1 Description of a locally two-dimensional vortex pair in the field of a transverse jet.

Viscosity is included in the model in the sense that the Gaussian viscous vortex structures are approximated as two contra-rotating Rankine vortices (solid-body rotation plus potential vortex). The local two-dimensional velocity distribution for the vortex pair is then represented in terms of $a(t)$, the radius of each viscous core, $\Gamma_0(t)$, the total (integrated) vortex strength associated with each vortex structure, and $h(t)$, the half-spacing of the vortices. Because the cross-flow velocity relative to the vortex pair changes with time [$U(t) = U_\infty \sin\phi_v(t)$], the extended Blasius theorem for unsteady, inviscid flow over a body whose size varies with time is used to compute the unsteady forces acting on each viscous core. Based on a "lift" force acting to separate the vortices, an ordinary differential equation for the vortex pair half-spacing $h(t)$ can then be derived and solved numerically based on formulation of $a(t)$, $\Gamma_0(t)$ and the initial conditions.

The assumption of the pair of Rankine vortices leads quite naturally to the representation for viscous core radius as $a(t) \sim \sqrt{\nu_t t}$. However, because the transverse jets under consideration are turbulent in general, an average eddy viscosity can be used in the expression for $a(t)$. As described in Ref. 11, for the range of actual Reynolds numbers applicable here ($Re = U_j d/\nu \cong 10{,}000$), eddy viscosities of several orders of magnitude greater than the kinematic viscosity yield little difference in the results obtained.

The variation in vortex strength Γ_0 is modeled here by accounting for a near-field component of vorticity arising from the deflected cross flow about the circular orifice,[12] as well as a far field component arising from vorticity generated by the jet's impulse. Cross-sectional slices of the jet taken downstream will then reveal both components of vorticity, contributing to the local circulation based on the local angle of orientation of the vortex pair $\phi_v(t)$. The analytical expression used in the present model is

$$\Gamma_0(t) = (2U_\infty d)\sin\phi_v(t) + \frac{P}{2\rho h(t)}\cos\phi_v(t) \quad (1a)$$

where P represents the jet impulse per unit depth. It should be noted that this expression is simply meant to be a reasonable correlation for Γ_0 based on important phenomena contributing to vorticity generation. In dimensionless form, the circulation takes the form

$$\tilde{\Gamma}_0(\tilde{t}) = \frac{\Gamma_0}{U_\infty L} = \frac{\pi^2/2}{\left[(4\pi\tilde{h} - 2/R)^2 + (\pi/8\tilde{h})^2\right]^{\frac{1}{2}}} \quad (1b)$$

where

$$\tilde{h}(\tilde{t}) \equiv h(t)/L, \quad \tilde{t} \equiv U_\infty t/L, \quad R \equiv U_j/U_\infty$$

and $L = Rd$ is the "characteristic length" for the problem.

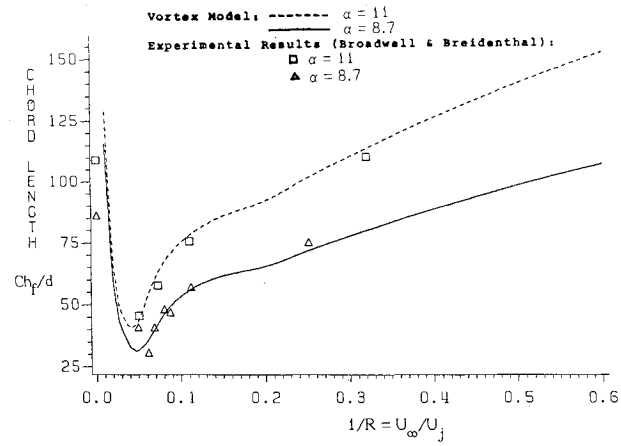

Fig. 2a Dimensionless flame chord length Ch_f/d as a function of velocity ratio U_∞/U_j for equivalence ratios α = 11 and 8.7.

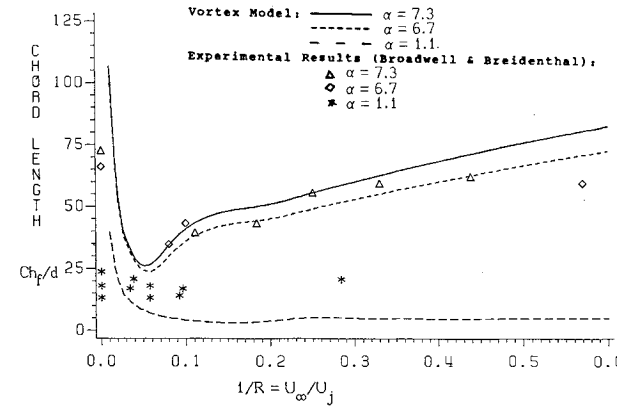

Fig. 2b Dimensionless flame chord length Ch_f/d as a function of velocity ratio U_∞/U_j for equivalence ratios α = 7.3, 6.7, and 1.1.

Initial conditions for the vortex half-spacing $h(t)$ are determined by the approximation that the recirculation cell represents the actual jet cross section in the far field. Extrapolating this assumption back to the vicinity of the jet orifice, an estimate on the cell area (and thus h) at the orifice, where dimensionless flow time is $\tilde{t}_0$, can be made. The ordinary differential equation for $\tilde{h}(\tilde{t})$, resulting from the force balance on the viscous cores, finally takes the form

$$\frac{d^2\tilde{h}}{d\tilde{t}^2} + \left(\frac{k+1}{k}\right)\frac{1}{\tilde{t}}\frac{d\tilde{h}}{d\tilde{t}} - \frac{\tilde{\Gamma}_0^2(\tilde{t})}{8\pi^2 k\tilde{h}^3(t)}\left[1 - \frac{C^2\tilde{t}}{(Re)\tilde{h}^2(\tilde{t})}\right] = 0 \quad (2)$$

with the initial condition

$$\tilde{h}(\tilde{t}_0) = \frac{1}{R}\left(\frac{\pi}{16B}\right)^{\frac{1}{2}}$$

and where $B = 2.84$ is a constant based on the area of the recirculation cell,[13] $C = 1.121$ a constant of proportionality relating core radius $a(t)$ to $\sqrt{4\nu_t t}$, and k the virtual mass coefficient for motion of the viscous core, approximated here as a constant for the entire trajectory and, as justified in Ref. 11, found to be equal to 4 for the present flowfield.

Once solution for the vortex half-spacing is obtained, correlation between flow time t and the location of the vortex pair in the flowfield can be found through a suitable representation of the local velocity of fluid along the vortex curve. Based on momentum conservation along the jet, a boundary-layer type of evaluation leads to the following governing equation for $\tilde{u}_v \equiv u_v/U_j$, the dimensionless mass-averaged velocity along

the jet trajectory:

$$\frac{d\tilde{u}_v}{d\tilde{t}} = \left[\frac{\cos\phi_v(\tilde{t}) - R\tilde{u}_v(\tilde{t})}{2R - \cos\phi_v(\tilde{t})/\tilde{u}_v(\tilde{t})}\right]\frac{2}{\tilde{h}(\tilde{t})}\frac{d\tilde{h}}{d\tilde{t}} \tag{3}$$

Transverse Fuel Jet Model

Based on the foregoing description, the situation in which the jet fluid and crossflow mix and react to form products of combustion now can be considered. Identified are several fundamental processes that govern the degree to which the reactants form products and, ultimately, the distance at which the "flame" ends. By definition, molecular diffusion of the fuel and oxidizer at the diffusion flame surface causes formation of combustion products and local depletion of the available fuel. Large-scale mixing and entrainment of the oxidizer into the vicinity of the jet also takes place downstream of the injection and can be visualized in terms of flame distortion and winding by the vortex pair structure (cf, Ref. 14). In addition, the heat transfer in the flame region caused by the buoyancy and radiation affects the flame length and structure as a result of the coupling of the energy and momentum conservation equations.

In his semiempirical modeling of the turbulent diffusion flame in a cross flow, Brzustowski[7] suggests that entrainment and buoyancy play key roles in solution of the flame shape and length, while radiation is of lesser importance. Broadwell and Breidenthal[5] argue, on the basis of far-field scaling laws, that for large jet Reynolds numbers entrainment is a dominant factor in determining flame length. Their scaling of the fuel jet far downstream of injection (i.e., for a relatively large cross-flow velocity U_∞) is predicted fairly well: but, as U_∞ is decreased and the case of the turbulent free jet is approached, the "transitional" behavior of the flame length observed in experiments cannot be predicted. The following analysis, which implements the transverse jet model, attempts to examine the role that entrainment plays in the reacting jet and to predict, to an extent, both the near- and far-field flame shapes and lengths.

In analogy to the transverse jet model, it is assumed that the cross section of the fuel jet is represented by the recirculation cell of the vortex pair. According to Brzustowski,[7] the effect of the vortex pair on the flame structure is quite pronounced at high jet-to-cross-flow velocity ratios and, in fact, flame length may be correlated[5] with the spacing of the vortices in the far field. Incompressibility is also assumed at present, even though the effects of heat release and buoyancy can be significant to the actual transverse diffusion flame. This is done so that the effects of large-scale entrainment can be isolated here and thus allows comparison with liquid experiments. Other assumptions made in the present model include negligible radiation effects and fast reaction kinetics, so that the rate of reactant consumption is limited only by the rate of entrainment of oxidizer.

Based on the foregoing considerations, it is postulated that a deflected flame of mixture ratio α ends when the flux of a molecularly mixed fluid in the jet is proportional to the amount of oxidizer entrained in the jet and the amount of fuel initially present in the jet cross section. In terms of the volume flux at the orifice, this is represented by

$$\frac{\text{Mass flux of mixed fluid in jet}}{\text{Initial mass flux of jet fluid}} = \frac{\rho\left[4Bh^2(t_*)\right]u_v(t_*)}{\rho\left[\frac{\pi}{4}d^2\right]U_j} = (E\alpha + 1) \tag{4}$$

where t_* is the flow time at which the flame ends, $4Bh^2(t)$ the area of the recirculation cell, $u_v(t)$ the mass-averaged jet velocity, ρ the jet (or cross-flow) density, and E a coefficient representing the amount of excess oxidizer entrained into the flame region which is required to put out the flame. If simple mixing were involved solely in the combustion process, E would be equal to unity and every element of jet fluid would need to be mixed with α parts of cross flow. Because of the significance of macroscopic mixing due to the coherent turbulent (vortical) flow structures and the "incompleteness of mixing or homogeneity in the flame" described by Hottel and Luce,[6] the actual value of E will exceed unity. Weddell's experiments for incompressible free jet mixing yield $E = 1.9$, the work of Steward[15] gives a value of $E = 4$ for the buoyant turbulent diffusion flame, and Brzustowski suggests a value of $E = 5.7$ for the transverse turbulent fuel jet. For the present, we will determine the value of E relevant to the cold transverse (incompressible) reacting jet by a comparison of our analytical calculations with the Broadwell-Breidenthal experimental flame length measurements. It will become clear that the functional dependence of flame length on the velocity ratio $R = U_j/U_\infty$ will be similar for different values of E; the more accurate numerical value will simply give a more appropriate magnitude for the flame length.

The procedure for the calculation of flame length as a function of α and R can be described as follows. At each value of $\tilde{t}$, the vortex pair spacing $\tilde{h}(\tilde{t})$ and local axial velocity $\tilde{u}_v(\tilde{t})$ are computed by solution of Eqs. (2) and (3) using a fourth-order Runge-Kutta numerical scheme. When Eq. (4) is satisfied (for a given value of E), the corresponding dimensionless time $\tilde{t}_*$ is used to solve for the location of the vortex pair in the flowfield (X_f and Z_f) at which the flame ends as follows:

$$\frac{X_f}{d} = R^2\int_{\tilde{t}_0}^{\tilde{t}_*}\tilde{u}_v(\tau)\cos\phi_v(\tau)\,d\tau \tag{5a}$$

$$\frac{Z_f}{d} = R^2\int_{\tilde{t}_0}^{\tilde{t}_*}\tilde{u}_v(\tau)\sin\phi_v(\tau)\,d\tau \tag{5b}$$

Broadwell and Breidenthal[5] approximate the flame length in their measurements by the chord length $Ch_f = \sqrt{X_f^2 + Z_f^2}$; here, Ch_f will be calculated for comparison.

This procedure yields results for the flame length given finite values of velocity ratio R. As the velocity ratio approaches infinity (that is, as the cross-flow velocity U_∞ decreases to zero), we approach the situation where a turbulent fuel jet is injected into a still reservoir of oxidizer, the case studied in liquid by Weddell. While the current model involving the viscous vortex pair is actually relevant only to the case of a nonzero cross-flow velocity, it is of interest to determine the asymptotic behavior of the governing equations as U_∞ approaches zero. The resulting dependence of flame length on the characteristic parameters can then be compared with experimental results in liquid.

In the limit as U_∞ becomes very small, a number of simplifications may be made. If we let $R = U_j/U_\infty \gg 1$, the expression for the deflection angle ϕ_v is simplified such that the total dimensionless circulation $\tilde{\Gamma}_0(\tilde{t})$ reduces to

$$\tilde{\Gamma}_0(\tilde{t}) = 4\pi\tilde{h} \tag{6}$$

since $4\pi\tilde{h} \ll \pi/8\tilde{h}$ and $\pi/8\tilde{h} \gg 2/R$ in this regime. It should be noted that, in dimensional terms, Eq. (6) becomes $\Gamma_0(t) = U_\infty[4\pi h(t)]$, which approaches zero as the cross-flow velocity $U_\infty \to 0$. Incorporation into the governing (force balance) equation (2) in $\tilde{h}(\tilde{t})$ gives an approximate solution for dimensionless half-spacing as a function of flow time,

$$\tilde{h}(\tilde{t}) = b\tilde{t}, \quad b = \left[\frac{2}{k+1}\right]^{\frac{1}{2}} \tag{7}$$

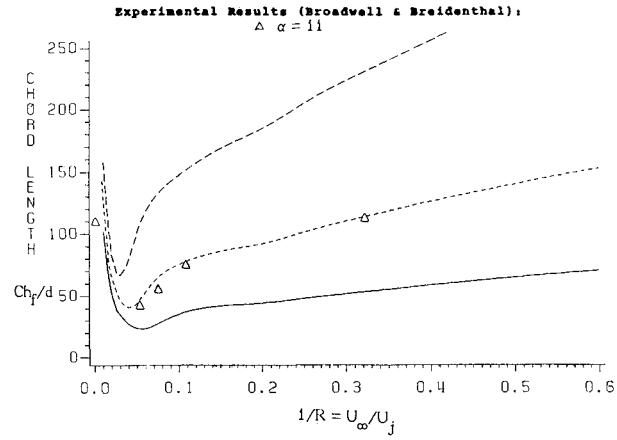

Fig. 3 Comparison of calculated flame length distributions for entrainment coefficients $E = 8$ (— — —), $E = 5$ (------), and $E = 3$ (———) (equivalence ratio $\alpha = 11$).

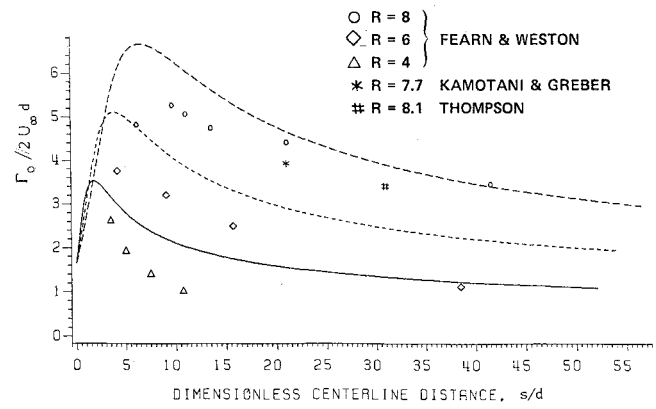

Fig. 4 Dimensionless circulation $\Gamma_0/2U_\infty d$ as a function of dimensionless arc length s/d for $R = U_j/U_\infty = 8$ (– – –), 6 (------), and 4 (———).

Based on this reasoning, Eq. (3) in axial velocity can be reduced to yield the following behavior as $U_\infty \to 0$:

$$\tilde{u}_v = \tilde{t}_0/\tilde{t}$$

The condition representing the flame end [Eq. (4)] can now be estimated. When $\tilde{t}_*$ is substituted to give the flame arc length s_f, we find that

$$\frac{s_f}{d} = R^2 \int_{\tilde{t}_0}^{\tilde{t}_*} \tilde{u}_v(\tau)\, d\tau = R\left[\frac{(k+1)\pi}{32B}\right]^{\frac{1}{2}} \ell n\,(E\alpha + 1) \quad (8)$$

Clearly, this behavior indicates that if $R \to \infty$ (or $U_\infty \to 0$), the flame length $s_f \to \infty$, in contrast to the finite flame lengths that are physically possible and observed by Weddell. Hence, there must exist an upper limit to the size of R such that the above analysis (and indeed, the entire model) is appropriate.

This limit is found by noting that for Eq. (6) to be a valid approximation for Γ_0 at high velocity ratios, $4\pi\tilde{h} \ll \pi/8\tilde{h}$. If substitution into this condition is made, with $\tilde{h} = b\tilde{t}_*$ and solution for $\tilde{t}_*$ and $\tilde{t}_0$ based on the flame end and orifice conditions, the following condition for the validity of Eqs. (6-8) emerges:

$$R \gg (E\alpha + 1)[2\pi/B]^{\frac{1}{2}} = R_L \quad (9)$$

Hence, for values of velocity ratio R satisfying the requirement of Eq. (9), the limiting relation [Eq. (8)] holds, indicating that actual vortex circulation vanishes and flame lengths become infinite. Clearly, the present model only can be used appropriately for values of $R \le R_L$. These values are calculated here.

Results and Discussion

Following the procedure outlined in the previous section, we can numerically solve the flame length and shape as functions of the velocity ratio R for several different values of equivalence (or mixture) ratio α. The approximate dimensionless flame (chord) length Ch_f as a function of $1/R = U_\infty/U_j$ is shown in Fig. 2, compared with Broadwell and Breidenthal's experimental findings.[5] It appears that a very clear correspondence exists between predicted and experimental points when the value of the entrainment coefficient is chosen to be $E = 5$. The "transition" in the behavior of flame length at values of U_∞/U_j below approximately 0.05 is predicted by our model, such that flame length decreases from a finite value at $1/R$ near zero to a minimum at $1/R = 0.05$ (the value is 0.04 for $\alpha = 11$). Figure 3 demonstrates the effect on chord length of varying E, indicating a shift in the magnitude of flame length but the same general shape of the curve. As noted by Broadwell and Breidenthal,[5] the flame lengths for $\alpha = 1.1$ do not follow the pattern as closely, since the flame lengths are too short to be described by far-field analysis. Since the present model does include near-field effects, it is shown that this lower equivalence ratio case is roughly predicted as well.

Table 1 Local circulation and deflection angle for flame end as compared with maximum circulation and corresponding deflection angle for $\alpha = 11$

		Flame end		Max. circulation	
$\frac{U_\infty}{U_j} = \frac{1}{R}$	$\frac{s_f}{d}$	$\frac{\Gamma_0(t_*)}{2U_\infty d}$	$\sin\phi_v(t_*)$	$\frac{\Gamma_0(t_m)}{2U_\infty d}$	$\sin\phi_v(t_m)$
0.02	50.95	280.6	0.9714	409.4	0.7072
0.03	37.68	257.8	0.8603	274.3	0.7135
0.04	37.27	203.0	0.6145	206.6	0.7086
0.05	46.00	133.6	0.3523	166.1	0.7170
0.06	56.26	88.4	0.2129	139.0	0.7155

The reason for there being the different locations observed in the flame length minimum (depending on α) is evident in the limiting condition on velocity ratio R given in Eq. (9). When $E = 5$, the minimum in $1/R$ depends on the equivalence ratio α, yielding $1/R_L = 0.012$ for $\alpha = 11$, $1/R_L = 0.018$ for $\alpha = 6.7$, and $1/R_L = 0.112$ for $\alpha = 1.1$. Since the minimum value of velocity ratio for which the model is valid *increases* with decreasing α, it follows that the value of $1/R$ at which the flame length minimum occurs should have the same behavior.

The observed transition in the flame length behavior for values of α exceeding unity has not been predicted well by other theoretical models, indicating that the present model constitutes a significant advance in our understanding of the phenomena governing near-field flame behavior. Clearly, this structural transition as U_∞ is increased is associated with the formation of the contra-rotating vortex pair at the jet orifice, a situation that is modeled somewhat more accurately by the present representation than by other "far-field" types of models. With reference to Fig. 4, which describes the downstream variation in circulation for the model, the fundamental phenomena related to fuel consumption by the flame can be assessed as outlined in the following paragraphs.

As the velocity of the cross flow is increased from zero, the jet proceeds into the cross flow, but is deflected relatively slowly in comparison to jet turning when U_∞ is of larger magnitude. Based on the modeling of Eq. (1a), as the jet turns,

the vorticity associated with the fuel jet increases, mixing becomes more rapid, and the flame is ultimately extinguished. As the ratio $1/R$ is increased to 0.05 (or R decreased to 20), apparently the circulation approaches its maximum more quickly and the dramatic rise in mixing causes the flame to be extinguished more quickly, giving a shorter flame length. As the ratio $1/R$ continues to increase beyond 0.05, the maximum circulation is smaller in magnitude and, as the jet is deflected more significantly, mixing increases and then decreases as the maximum $\Gamma_0(t)$ is passed. The flame is then extinguished at a greater arc length s_f (or chord length Ch_f) when sufficient mixing has taken place.

These suggestions are borne out by documentation of the local values of deflection angle $\phi_0(t)$ and circulation $\Gamma_0(t)$ at the point where a given flame ends. As Table 1 indicates for an equivalence ratio $\alpha = 11$, when $1/R$ is less than the "transition" value 0.04, the flame is extinguished before the circulation has reached its maximum. When $1/R = 0.04$, the circulation is close to its maximum when the flame ends and, when $1/R > 0.04$, the maximum circulation has passed and Γ_0 is a *decreasing* function when the flame ends.

The present results in addition corroborate the far-field flame length predictions made by Broadwell and Breidenthal,[5] who find that for mixture ratios significantly greater than unity, the far-field behavior is

$$\frac{X_f}{d} \sim \left[\frac{\pi}{4R}\right]^{\frac{1}{2}} (\alpha + 1)^{\frac{3}{2}} \tag{10}$$

As a comparison with Broadwell and Breidenthal's observed axial flame length, Fig. 5 presents a nondimensionalized description of X_f as a function of velocity ratio $1/R$ for cases where $\alpha \gg 1.1$. Clearly, the far-field equation (10) is appropriate for values of $1/R$ exceeding 0.1; the near-field description contained in the present model is needed for prediction where $0.01 < 1/R < 0.1$.

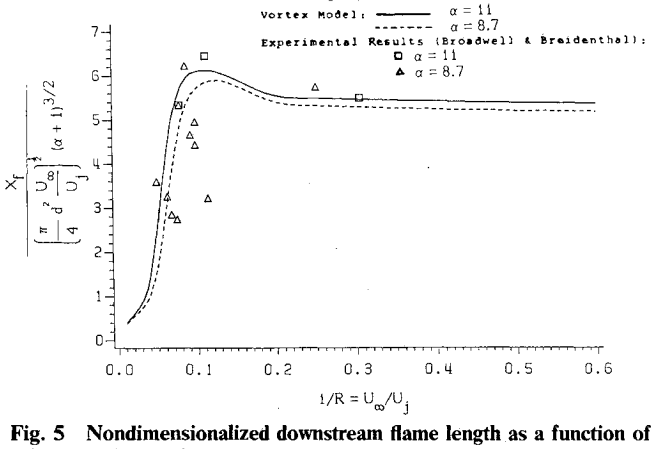

Fig. 5 Nondimensionalized downstream flame length as a function of velocity ratio U_∞ / U_j.

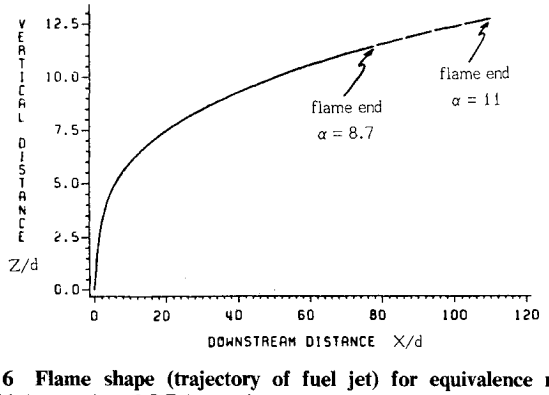

Fig. 6 Flame shape (trajectory of fuel jet) for equivalence ratios $\alpha = 11$ (- - - -) and 8.7 (——).

Results for flame shapes, i.e., Z/d vs X/d until Z_f and X_f are reached, are given in Fig. 6 for selected values of equivalence ratio. The far-field behavior of many of these flames can be described by the scaling law

$$Z/d = \alpha(R)^{\beta}(X/d)^{\gamma}$$

where $\alpha = 0.53$, $\beta = 1.18$, and $\gamma = 0.31$. This corresponds very roughly to the experimental cold-jet results of Pratte and Baines,[16] where $\alpha = 2.05$, $\beta = 0.72$, and $\gamma = 0.28$. Brzustowski et al.[10] confirm this scaling law as a far-field approximation to the hydrogen diffusion flame in a cross flow; however, if the present model were modified to account for buoyancy and density variation effects, it is likely that scaling coefficients different from those obtained here would result.

Conclusions

This analytical vortex model for the transverse reacting jet predicts quite well the behavior and length of the resulting flame structure in the absence of heat release effects. In particular, the sharp minimum in flame length observed in experiments is seen here to occur at $U_\infty/U_j = 0.05$ for a variety of liquid reaction equivalence ratios. The transformation in flow structure that accounts for this minimum arises from the change in the dominant component of vorticity near the jet orifice as compared with that in the far field. In addition, it is observed that, at the flame tip, the ratio of oxidizer entrained by the jet to fuel present in the jet is of the order of 5. It is postulated that this arises due to the large-scale flame distortion and mixing imposed by the vortex structures that results in the regions of unmixed reactants within the jet cross section.

While the model best predicts the behavior of a transverse reacting jet in a liquid system where the density variations are negligible, as a preliminary result we may infer that the flame shape in a gaseous reaction behaves roughly in the same way, with a dominance of entrainment effects. Examination of the effects of buoyancy for the transverse diffusion flame is planned for future studies.

Acknowledgments

The author wishes to express appreciation to Mr. Trinh Nguyen for performing the numerical work for the fuel jet computations. This work is supported in part by the National Science Foundation under Research Initiation Grant MEA 83-05960 and by the National Aeronautics and Space Administration under Grant NAG 3-543.

References

[1] Keffer, J. F. and Baines, W. D., "The Round Turbulent Jet in a Cross-Wind," *Journal of Fluid Mechanics*, Vol. 15, 1963, pp. 481-496.

[2] Kamotani, Y. and Greber, I., "Experiments on a Turbulent Jet in a Cross Flow," *AIAA Journal*, Vol. 10, Nov. 1972, pp. 1425-1429.

[3] Fearn, R. and Weston, R. P., "Vorticity Associated with a Jet in a Cross Flow," *AIAA Journal*, Vol. 12, Dec. 1974, pp. 1666-1671.

[4] Le Grives, E., "Mixing Process Induced by the Vorticity Associated with the Penetration of a Jet into a Cross Flow," *Journal of Engineering for Power*, Vol. 100, July 1978, pp. 465-475.

[5] Broadwell, J. E. and Breidenthal, R. E., "Structure and Mixing of a Transverse Jet in a Cross Flow," *Journal of Fluid Mechanics*, Vol. 148, 1984, pp. 405-412.

[6] Hottel, V. O. and Luce, R. G., "Burning in Laminar and Turbulent Fuel Jets," *Fourth Symposium (International) on Combustion*, Williams and Wilkins Co., Baltimore, MD, 1953, p. 97.

[7] Brzustowski, T. A., "Hydrocarbon Turbulent Diffusion Flame in Subsonic Cross Flow," *AIAA Progress in Astronautics and Aeronautics*:

Turbulent Combustion, Vol. 58, edited by L. A. Kennedy, AIAA, New York, 1977, pp. 407-430.

[8]Hoehne, V. O. and Luce, R. G., "The Effect of Velocity, Temperature, and Molecular Weight on Flammability Limits in Wind-Blown Jets of Hydrocarbon Gasses," American Petroleum Institute Paper, 56-70, 1970.

[9]Brzustowski, T. A., "Flaring in the Energy Industry," *Progress in Energy and Combustion Science*, Vol. 2, No. 3, 1976, pp. 129-141.

[10]Brzustowski, T. A., Gollahalli, S. R., and Sullivan, H. J., "The Turbulent Hydrogen Diffusion Flame in a Cross-Wind," *Combustion Science and Technology*, Vol. 11, 1975, pp. 29-33.

[11]Karagozian, A. R., "An Analytical Model for the Vorticity Associated with a Transverse Jet," *AIAA Journal*, Vol. 24, April 1986, pp.

[12]Chang-Lu, H., "Aufrollung unes Zylindrischen Strahles durch Overwind," Ph.D. Dissertation, University of Göttingen, FRG, 1942.

[13]Lamb, H., *Hydrodynamics*, 6th ed., Dover Publications, New York, 1945.

[14]Gollahalli, S. R., Brzustowski, T. A., and Sullivan, H. F., "Characteristics of a Turbulent Propane Diffusion Flame in a Cross-Wind," *Transactions, Canadian Society for Mechanical Engineering*, Vol. 3, No. 4, 1975, pp. 205-214.

[15]Steward, F. R., "Prediction of the Height of Turbulent Diffusion Buoyant Flames," *Combustion Science and Technology*, Vol. 2, 1970, pp. 203-212.

[16]Pratte, B. D. and Baines, W. D., "Profiles of the Round Turbulent Jet in a Cross Flow," *Proceedings of ASCE, Journal of the Hydraulics Division*, Nov. 1967, pp. 56-63.

[17]Thompson, A. M., "The Flow Induced by Jets Exhausting Normally from a Plane Wall into an Airstream," Ph.D. Thesis, University of London, 1971.